THERMAL CONDUCTIVITY OF VACUUM – SCREEN HEAT INSULATION

D. P. Lebedev, E. K. Zlobin,
and V. V. Alekseev

UDC 536.21

Experimental data for the thermal conductivity parallel to the layers of vacuum–screen insulation at various temperatures and vacua of $760\text{-}5 \cdot 10^{-7}$ mm Hg are given. The anisotropy of the thermal conductivity is determined.

Most investigations of the thermal conductivity of vacuum–screen (multilayer) heat insulation (VSHI) have been concerned with the thermal conductivity normal to the layers [1-5]. In most cases the investigators have determined some effective thermal conductivity, the value of which gives an idea of the mechanism of heat transfer in the laminated VSHI system. The engineering use of VSHI in various installations and the calculation of heat fluxes, however, necessitate a fuller understanding of the mechanism of heat transfer in this system and a determination of specific values of the thermal conductivity in a wide range of vacua. We believe it worthwhile to consider the mechanism of heat transfer by thermal conduction in VSHI normal to ($\lambda_\perp$) and along (parallel to) the layers ($\lambda_\parallel$).

According to the hypotheses of various authors, the thermal conductivity along the layers in VSHI may differ from the thermal conductivity normal to the layers by a factor of hundreds. This indicates considerable anisotropy of the thermal conductivity of a system such as VSHI.

At present we have no data on thermal conductivity along VSHI layers. In the best case we have information about the thermal conductivity along a single layer of insulation, determined by the square method without inclusion of the radiative component due to reemission along the layers [1].

An attempt was made in [7] to evaluate the thermal conductivity parallel to insulating layers from the thermal conductivity along layers of a cylindrical specimen of such insulation. For these tests the authors adapted a low-temperature thermal conductivity apparatus and obtained data for the thermal conductivity of Mylar superinsulation at a pressure of 10^{-7} torr.

In the present paper we describe an apparatus which can be used to determine the thermal conductivity along the layers ($\lambda_\parallel$) of vacuum–screen insulation in the pressure range from 10^{-7} to 10^{-1} mm Hg for several boundary temperatures. In the light of the obtained results for the thermal conductivity along the layers ($\lambda_\parallel$) and data for the thermal conductivity normal to the layers ($\lambda_\perp$) [8], we discuss the mechanism of heat transfer in the laminated VSHI system.

EXPERIMENTAL METHOD

The effective thermal conductivity along the layers ($\lambda_\parallel$) of multilayer insulation was determined from the thermal conductivity of a cylindrical specimen formed by rolling up a piece of the investigated multilayer insulation. We used the steady-state method for a infinite plane layer with the known expression for the thermal conductivity

$$\lambda_\parallel = \frac{Q}{t_1 - t_2} \cdot \frac{\delta}{F} \quad \text{W/m·deg.} \tag{1}$$

Moscow Institute of Chemical Engineering. Translated from Inzhenerno-Fizicheskii Zhurnal, Vol. 21, No. 5, pp. 789-796, November, 1971. Original article submitted March 18, 1971.

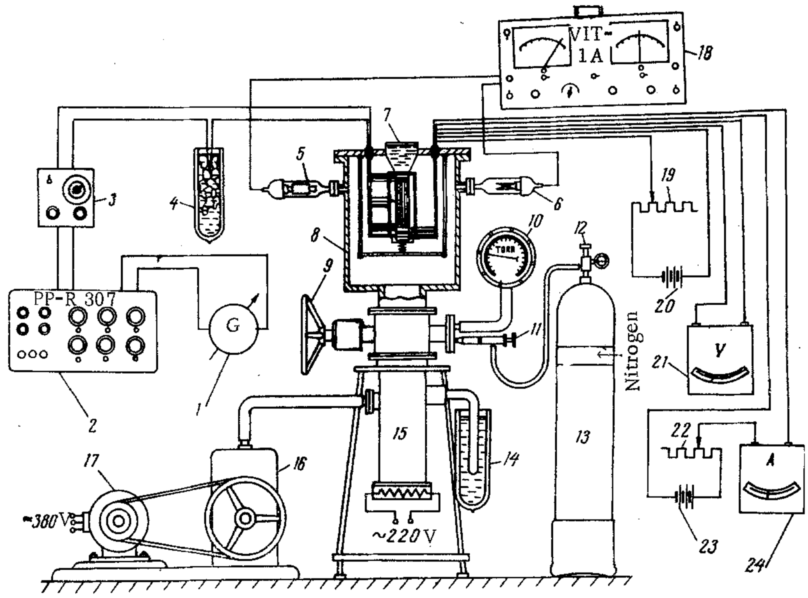

Fig.1. Diagram of experimental apparatus. 1) M 195/3 null galvanometer; 2) R 307 potentiometer; 3) switching device; 4) Dewar vessel; 5) LM-2 pressure gage; 6) LT-2 pressure gage; 7) cooled reservoir; 8) vacuum chamber; 9) vacuum lock; 10) torr vacuum gage; 11) needle leak; 12) reducer; 13) gas cylinder; 14) nitrogen trap; 15) N-1S-2 diffusion pump; 16) VN-461M forepump; 17) electric motor; 18) VIT-1A vacuum gage; 19) guard heater rheostat; 20) guard heater battery; 21) D502 voltmeter; 22) R33 resistance box; 23) main heater battery; 24) D502 ammeter.

Henceforth we will regard $\lambda_{\|}$ as the thermal conductivity obtained with particular temperature boundary conditions on the specimen.

Experimental Apparatus

A complete diagram of the experimental apparatus is shown in Fig.1. The apparatus enabled us to determine the effective thermal conductivity along layers of multilayer insulation in the temperature range -190°C to $+120$°C in a wide range of vacuum up to $5 \cdot 10^{-7}$ torr.

The required operating pressure in the vacuum chamber was obtained by the admission of gaseous nitrogen through the needle valve 11. We chose nitrogen as the gas to ensure that there was no condensation of the gas on the low-temperature surfaces of the test specimen.

The heat conditions became steady within 8-14 h of the start of cooling of the specimen. This time could be reduced by cooling the specimen at a higher pressure than that required in the experiment.

The main component of the experimental apparatus was the calorimeter shown in Fig.2.

The test specimen 2, in the form of a cylinder 165 mm long and 26 mm in diameter, was mounted vertically between two thermostatted surfaces. The specimen was made of 12 μ thick polyethylene terephthalate film, aluminized on one side, and embossed on a 0.5 × 2 mm grid. The packing density of the specimen was 13 layers/mm.

The experimental specimen for the investigations was made by rolling up a continuous strip of the metallized film until a specimen of the required diameter was obtained. A gap between the film layers was produced by the insertion of spacing strips of annealed copper foil, which were rolled up with the metallized film. The spacing foil strips were 5 mm wide and were situated at the ends of the specimen. By low-temperature soldering of the ends of the specimen we obtained highly conducting solid end plates in good contact with the layers of insulation. These ends were subsequently ground down to a thickness of 2.5 mm. Copper–Constantan 0.1 mm thermocouples were embedded in the plane-parallel ends of the specimen. When the heat flux through the specimen was low the temperature drop in the end plates was neglected.

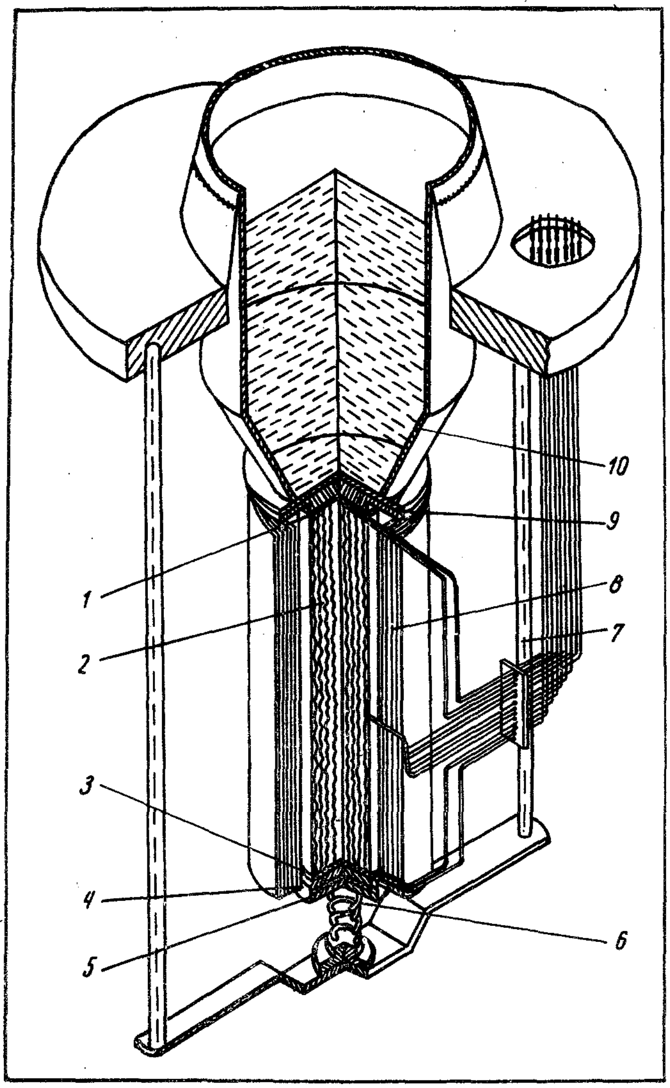

Fig. 2. Calorimeter: 1) upper heat flux gage; 2) test specimen; 3) heat flux gages; 4) main heater; 5) guard heater; 6) spring; 7) thermocouple and electric lead-ins; 8) screen; 9) removable washer; 10) cooled reservoir.

The temperature of the cold upper surface was kept constant using liquid nitrogen, solid carbon dioxide, or melting ice, placed in the cooled reservoir 10, which was made of industrial copper sheet. The cooled reservoir was silver-soldered to a conical skirt of 1Kh18N9T sheet steel, which was welded to the top flange of the vacuum chamber. The level of the cooling liquid was checked visually. The heat influx to the cooling reservoir was low owing to the high thermal resistance of the thin-walled stainless steel skirt and the low emissivity of the polished walls of the copper reservoir. The temperature of the lower thermostatted surface was kept constant by the main heater 4. In our experiments it was 30°C. Between the test specimen and the thermostatted surfaces there were lower (1) and upper (3) heat-flux gages to measure the heat fluxes entering and leaving the ends of the specimen.

For heat-flux measurement we used the heat-flux gages devised and constructed by the Kiev Institute of Technical Thermophysics, Academy of Sciences of the Ukrainian SSR. These consist of numerous differential thermocouple junctions connected in series and forming a cylinder 26 mm in diameter and 2 mm high [6]. We improved the gages in such a way that the heat flux over the area of the gage was more uniform. The improved gages were calibrated again in vacuo on a special stand. The gages used in the present experiment had a sensitivity of 0.025-0.035 W/mV and were linear over the whole range of measured fluxes.

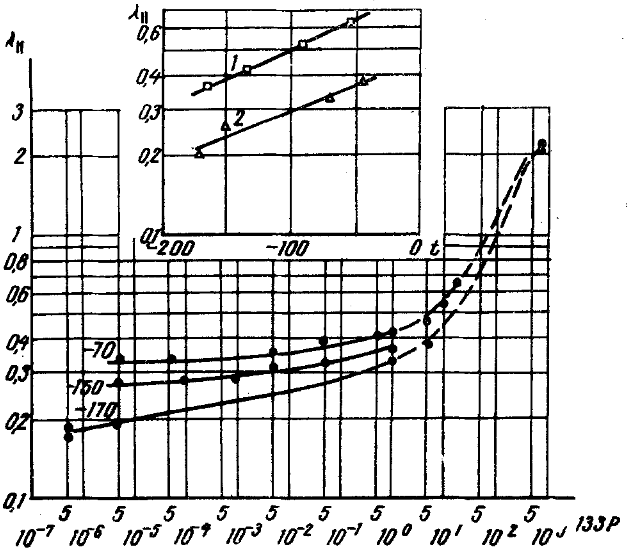

Fig.3

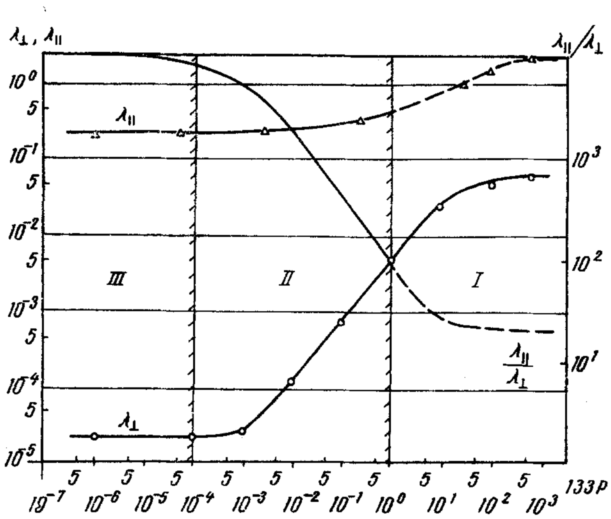

Fig.4

Fig.3. Thermal conductivity $\lambda_{\|}$, W/m·deg C along VSHI layers as a function of the pressure P, N/m^2, and the temperature of cold end of specimen t, °C: −70, −150, −170 are the temperatures of the cold end of the specimen; the black dots are the experimental points; 1) of [8]; 2) results of experiment at pressure $5 \cdot 10^{-6}$ mm Hg.

Fig.4. Anisotropy factor $N(\lambda_{\|}/\lambda_{\perp})$ of thermal conductivity for vacuum–screen insulation as a function of the pressure P: $\lambda_{\perp}$ is the thermal conductivity in the perpendicular direction; the points are the experimental data.

The heat-flux gages were attached to the ends of the test specimen by two methods: by the pressure of a calibrated spring 6, exerting a force of 5 kgf, after the contacting surfaces had been smeared with vacuum grease; or by application of epoxy resin to these surfaces. We found no differences in the obtained results.

The upper gage 1 was attached in a similar way to a removable washer 9 fitted to the bottom of the cooled reservoir 10. The removable washer was made of heat-insulating material and could have temperatures between those of liquid nitrogen and dry ice. The lower heat-flux gage 3 was attached by the same method to the main heater 4, which was in the form of a disk 26 mm in diameter and 2 mm thick. The industrial copper heater block contained a uniformly distributed Constantan electric heater which could develop a power of up to 15 W. Behind the main heater 4 there was a null flux gage 3, connected to a null galvanometer. Using the guard heater 5 we could ensure the absence of flux through the null gage to an accuracy of better than 0.002 W.

The heat-insulating screen 1, made of 20 layers of metallized 5 μ thick polyethylene terephthalate film, was attached by a band directly to the washer 9. The lower end of the screen rested freely on the compression spring 6. All the thermocouple and electric leads were brought through isothermal surfaces to exclude heat leakage through them.

According to our estimates, the error in the determination of $\lambda_{\|}$ in the vacuum range 10^{-1}–$5 \cdot 10^{-7}$ mm Hg was not more than 6%. At a vacuum lower than 10^{-1} mm Hg the error was much greater due to convective heat transfer.

Heat Transfer in Vacuum – Screen Insulation

The relationships illustrated in Fig.3 show that in the pressure range 10^{-7}–10^{-1} mm Hg the value of $\lambda_{\|}$ does not vary greatly and is close to the thermal conductivity of the film from which the VSHI screens were made. The increase in thermal conductivity with reduction of the pressure to 10^{-1} mm Hg indicates an increase in the gas conduction along the VSHI layers.

The sharp increase in $\lambda_{\|}$ at a pressure above 10 mm Hg (broken curve) indicates the presence of convective heat currents near the specimen and in the experimental apparatus in these conditions.

The top part of Fig. 3 shows the thermal conductivity along the layers ($\lambda_{\parallel}$) as a function of the temperature of the cold end of the specimen (at $P \simeq 5 \cdot 10^{-6}$ mm Hg). The obtained relationship 2 agrees well with 1, which is given for similar Mylar superinsulation in [8]. The increase in $\lambda_{\parallel}$ with temperature indicates the development of the radiative component.

Figure 4 shows the thermal conductivities $\lambda_{\perp}$ and $\lambda_{\parallel}$ as functions of pressure. The best idea of the anisotropy of the thermal conductivity in VSHI is given by the relationship $N(\lambda_{\parallel}/\lambda_{\perp}) = f(P)$. To plot this relationship we used the graph of $\lambda_{\perp} = f(P)$ from [8]. As shown by Fig. 4, the anisotropy of the thermal conductivity of vacuum–screen heat insulation, characterized by the ratio $\lambda_{\parallel}/\lambda_{\perp}$, is a variable value, which depends on the pressure, and was 10-10^4 for the investigated insulation.

The whole investigated vacuum range can be divided into several regions according to the behavior of the curve of $N(\lambda_{\parallel}/\lambda_{\perp}) = f(P)$ (see Fig. 4): I) the continuum region (760 mm Hg–1 mm Hg); II) the gas conduction region (1 mm Hg–10^{-4} mm Hg); III) the region of radiative and conductive conductivities (from 10^{-4} mm Hg).

In the region I the thermal conductivity of the gas filling the VSHI makes a significant contribution to the effective thermal conductivity. The dynamic behavior of the gas passing through the insulation in this region is determined both by continuous flow and by viscous slip flow.

With an increase in the vacuum in region II the amount of heat transferred by the conducting gas within the VSHI layers is greatly reduced. The region where the curve of $N(\lambda_{\parallel}/\lambda_{\perp}) = f(P)$ is a linear function of pressure (10^{-3} mm Hg–1 mm Hg) can be regarded as the region of free-molecular flow. If the pressure (region III) is reduced further below 10^{-3}–10^{-4} mm Hg, the thermal conductivity of VSHI approaches that of the solid framework of the insulation with the inclusion of the radiative contribution.

This analysis of the experimental results shows that an accurate assessment of the heat-insulating properties of vacuum–screen insulation necessitates a consideration of the specific features of the structure and the thermal conductivity of VSHI along the layers.

NOTATION

$\lambda_{\parallel}$ is the effective thermal conductivity along (parallel to) layers of vacuum–screen heat insulation;
$\lambda_{\perp}$ is the effective thermal conductivity normal to layers of vacuum–screen heat insulation;
Q is the heat flux through the test specimen;
t_1, t_2 are the temperatures on the ends of the test specimen;
δ is the distance between the ends of the specimen;
F is the cross-sectional area of the specimen;
P is the pressure (vacuum).

LITERATURE CITED

1. M. G. Kaganer, Heat Insulation in Low-Temperature Technology [in Russian], Mashinostroenie (1966).
2. R. S. Mikhal'chenko, A. G. Gerzhin, V. T. Arkhipov, N. P. Pershin, and L. V. Klipach, Inzh.-Fiz. Zh., 14, No. 1 (1968).
3. R. S. Mikhal'chenko, A. G. Gerzhin, and N. P. Pershin, Inzh.-Fiz. Zh., 11, No. 5 (1966).
4. R. S. Mikhal'chenko, A. G. Gerzhin, V. T. Arkhipov, and N. P. Pershin, Inzh.-Fiz. Zh., 16, No. 3 (1969).
5. R. S. Mikhal'chenko, V. F. Getmanets, and B. Ya. Sukharevskii, Inzh.-Fiz. Zh., 18, No. 3 (1970).
6. O. A. Gerashchenko and V. G. Fedorov, Heat and Temperature Measurements [in Russian], Naukova Dumka, Kiev (1965).
7. G. G. Androulakis and R. Kosson, J. Spacecraft and Rockets, 6, 841 (1969).
8. G. W. Anderson and G. F. Merlet, Chem. Eng. J., 62, No. 61 (1969).